# Experimental Investigation and Thermodynamic Modeling Assessment of the NaCl-NaI-$MgCl_2$-$MgI_2$ Quaternary System

Alders, Dennis C.; Rooijakkers, Bas A.S.; Konings, Rudy J.M.; Smith, Anna L.

**DOI**
10.1021/acs.jpcc.4c07788

**Publication date**
2025

**Document Version**
Final published version

**Published in**
Journal of Physical Chemistry C

THE JOURNAL OF PHYSICAL CHEMISTRY C
A JOURNAL OF THE AMERICAN CHEMICAL SOCIETY



pubs.acs.org/JPCC
Article

# Experimental Investigation and Thermodynamic Modeling Assessment of the NaCl−NaI−$MgCl_2$−$MgI_2$ Quaternary System

Dennis C. Alders, Bas A.S. Rooijakkers, Rudy J.M. Konings, and Anna L. Smith*

Cite This: J. Phys. Chem. C 2025, 129, 2726−2738
Read Online

ACCESS | Metrics & More | Article Recommendations | Supporting Information

**ABSTRACT:** The thermochemistry of the quaternary molten salt system NaCl−NaI−$MgCl_2$−$MgI_2$ has been studied using an experimental and thermodynamic modeling approach. The binary subsystems NaCl−NaI and NaCl−$MgCl_2$ were reassessed based on existing data in the literature. The binary subsystem NaI−$MgI_2$ was subjected to a renewed experimental investigation, to complement and revisit the data in the literature. The subsystem $MgCl_2$−$MgI_2$ was investigated for the first time in this work using Differential Scanning Calorimetry (DSC). Furthermore, the phase equilibria in the pseudobinary phase diagrams of NaCl−$MgI_2$ and NaI−$MgCl_2$ in the quaternary system were investigated by DSC, while the condensed phases in the quaternary system were investigated using X-ray diffraction (XRD). A thermodynamic model of the quaternary system was developed using the CALPHAD (CALculation of PHase Diagrams) method with the quadruplet approximation in the modified quasichemical model for the liquid phase, and two-sublattice polynomial models for the solid solution phases. With this model, the liquidus surface of the NaCl−NaI−$MgCl_2$−$MgI_2$ quaternary system has been described for the first time.

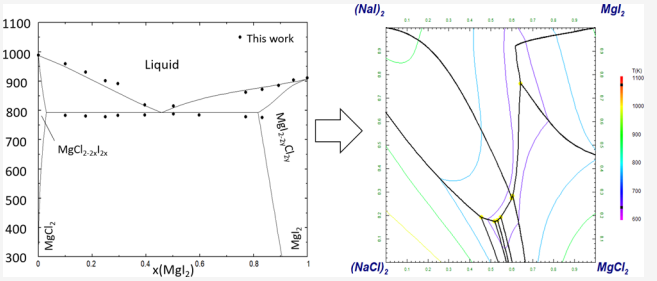


## 1. INTRODUCTION

Molten chloride salts are a class of materials that are central in the framework of fast neutron spectrum Molten Salt Reactor (MSR) development. In this type of nuclear reactor, chloride salts can be used as both fuel and coolant. The reason for this lies in their attractive qualities in terms of high thermochemical stability and low vapor pressures, even at elevated temperatures, and their high actinide solubility.[1,2] For a safety assessment of the MSR, a thorough understanding of the thermodynamic and thermo-physical properties of these salts is needed. The fuel system of interest in this work is the NaCl−$MgCl_2$−$PuCl_3$ salt system,[3,4] but for a full safety and longevity assessment, this system alone is not enough. During the fission reaction of the fissile $^{239}Pu$ in the fuel, the driving force that produces energy in a nuclear reactor, fission products are produced. These elements can dissolve in the molten salt fuel, and affect the thermochemical properties of the melt. Furthermore, these fission products pose a precipitation or volatilization risk, and therefore their behavior in the molten salt must be studied in detail.

A fission product that is of particular interest for the safety assessment of the MSR is iodine. In Light Water Reactors (LWRs)[5] and fluoride-based MSRs,[6,7] the effect of iodine on the thermochemical properties of the nuclear fuel has been investigated already. In particular in molten fluorides, iodine poses a volatility risk[7] in case the solubility limit of iodine in the melt is exceeded and CsI forms as an equilibrium phase. In this work, the addition of iodine to a molten chloride fuel has been investigated, starting with the effect it has on the binary NaCl−$MgCl_2$ system, which serves as the fuel matrix. This has been done by the investigation of the quaternary NaCl−NaI−$MgCl_2$−$MgI_2$ system. For this, a CALPHAD (CALculation of PHase Diagrams) model has been constructed based on data from the literature, as well as experimental data obtained in this work.

Experimental investigations using differential scanning calorimetry (DSC) and X-ray diffraction (XRD) have been performed to fill in the most important gaps that became evident after analyzing the data in the literature. Subsequently, CALPHAD models of the binary subsystems NaCl−NaI, NaCl−$MgCl_2$, NaI−$MgI_2$, and $MgCl_2$−$MgI_2$ have been developed. These models use the quasi-chemical formalism in the quadruplet approximation for the liquid solutions and a two-sublattice polynomial model for the solid solutions. The mixing enthalpy of the systems is also modeled, either based on experimental data or on the estimation method of Davis and Rice,[8] described in more detail in a previous work.[9] Furthermore, DSC and XRD investigations of the quaternary

Received: November 18, 2024
Revised: January 14, 2025
Accepted: January 14, 2025
Published: January 24, 2025

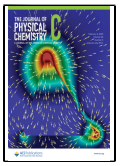







https://doi.org/10.1021/acs.jpcc.4c07788
J. Phys. Chem. C 2025, 129, 2726−2738

Table 1. End Member Specifications of the Salts Used in This Work

| end-member | supplier | reported purity | XRD analysis | $T_{melt}$ (K), DSC | $T_{melt}$ (K), lit. |
|---|---|---|---|---|---|
| NaCl | Thermo-Fischer | 99.998% | No visible impurities | 1074 ± 5 | 1073.8[10] |
| NaI | Thermo-Fischer | 99.999% | No visible impurities | 934 ± 5 | 933[10] |
| $MgCl_2$ | Thermo-Fischer | 99.998% | No visible impurities | 988 ± 5 | 987[10] |
| $MgI_2$ | Thermo-Fischer | 99.999% | No visible impurities | 911 ± 5 | 907[10] |

system have been performed through the binary systems NaI−$MgCl_2$ and NaCl−$MgI_2$, and the thermodynamic model has been optimized accordingly.

## 2. METHODS

**2.1. Experimental Techniques.** *2.1.1. Sample Preparation.* For the experiments carried out in this work, the end-members were used as delivered by the supplier. The purity of the end-members has been verified by XRD and DSC, as shown in Table 1. No secondary impurity phases were detected by DSC, and the measured melting temperatures were found in excellent agreement with the data in the literature. Due to the sensitivity of the salts toward oxygen and water, all sample preparation was carried out inside a glovebox under a dry argon atmosphere ($H_2O$, $O_2$ < 5 ppm).

Weighing was carried out using a Mettler-Toledo XPE105DR balance with a 0.01 mg uncertainty. Sample preparation was conducted by mixing end-members in the appropriate stoichiometric ratios in an agate mortar inside the dry argon atmosphere in the glovebox.

*2.1.2. X-ray Diffraction (XRD).* XRD measurements were carried out using a PANalytical X'pert pro diffractometer with a Cu-anode (0.4 mm × 12 mm line focus, 45 kV, 40 mA). Scattered X-ray intensities were measured with a real-time multistep detector (X'Celerator). The angle $2\theta$ was set to cover a range from 10 to 120°. Measurements were typically performed for 7−8 h, with a step size of 0.0036°/s. Refinement of the measured XRD data was performed by applying the method of Rietveld, Loopstra, and van Laar,[11,12] using the FullProf software, Version 5.10.[13]

*2.1.3. Differential Scanning Calorimetry (DSC).* The invariant temperatures in the investigated systems were measured using a Setaram multidetector high-temperature calorimeter (MHTC-96 type) equipped with a 3D heat flux DSC module, capable of measuring up to 1673 K. Sample preparation was done by mixing end-members NaCl, NaI, $MgCl_2$ and $MgI_2$ in the desired stoichiometric ratios. The samples were contained in a nickel liner, which in turn was inserted in a tightly closed stainless steel crucible.[14] Equilibration of the sample was done in the calorimeter itself during the first heating cycle by heating the mixtures to a temperature above the melting points of both end-members. Invariant equilibria were collected on the subsequent cycles.

The temperature was monitored throughout the experiments by a series of interconnected S-type thermocouples. The temperature on the heating ramp (10 K $min^{-1}$) was calibrated and corrected for the effect of the heating rate by measuring the melting points of standard high-purity metals (In, Sn, Pb, Al, Ag, Au) at 2−4−6−8−10−12 K $min^{-1}$. The calibration procedure was performed as recommended by Höhne et al.[15] and Della Gatta et al.[16] The transition temperatures in the investigated phase diagrams were derived on the heating ramp as the onset temperature using tangential analysis of the recorded heat flow. The liquidus temperature of mixtures was derived from the peak extremum of the last thermal event. The uncertainty on the measured temperatures is estimated to be ±5 K for pure compounds and ±10 K for mixtures.

**2.2. Thermodynamic Modeling.** The thermodynamic modeling assessment of the molten salt systems was performed with the CALPHAD method[17] using the FactSage software, Version 8.2.[18] Both literature and experimental data obtained in this work were used to adjust the excess parameters of the Gibbs energy functions of the phases present in the systems.

*2.2.1. Stoichiometric Compounds.* The Gibbs energy function for stoichiometric compounds is dependent on the standard enthalpy of formation ($\Delta_f H^\circ_m(298)$), the standard entropy ($S^\circ_m(298)$) at the reference temperature of 298.15 K, and the heat capacity ($C^\circ_{p,m}(T)$) as shown in eq 1 (with $T$ in K).

$$G(T) = \Delta_f H^\circ_m(298) - S^\circ_m(298)T + \int_{298}^{T} C_{p,m}(T)dT - T\int_{298}^{T} \frac{C_{p,m}(T)}{T}dT \quad (1)$$

The isobaric heat capacity $C_{p,m}$ is expressed as a polynomial that takes the form of eq 2.

$$C_{p,m}(T) = a + bT + cT^{-2} + dT^2 + eT^{1/2} \quad (2)$$

The compounds in the investigated systems are four end-members and four intermediates in the NaCl−$MgCl_2$ system. The thermodynamic data for all compounds are listed in Table 2. Thermodynamic data for NaI, $MgCl_2$, and $MgI_2$ were taken from the JANAF thermochemical database.[10] It should be noted that the heat capacities of NaI and $MgI_2$ as reported in the JANAF thermochemical database are estimated values, rather than experimental data. The thermodynamic data for NaCl was taken from van Oudenaren et al.,[19] as it was also used in our previous studies.[9,20−23] The heat capacities of intermediates $NaMgCl_3$ and $Na_2MgCl_4$ were taken from Chartrand et al.,[24] whereas their standard enthalpy of formation and standard entropy at 298 K were reoptimized in this work. The heat capacities of intermediates $Na_6MgCl_8$ and $Na_2Mg_3Cl_8$ were obtained using the Neumann-Kopp rule, and their standard enthalpy of formation and standard entropy at 298 K were optimized.

*2.2.2. Liquid Solution.* The excess Gibbs energy terms of the liquid solution are modeled using the quasi-chemical formalism in the quadruplet approximation, as proposed by Pelton et al.,[25] which has proven to be well-adapted to molten chloride and fluoride systems. This description assumes the existence of cation−anion quadruplets in the liquid, allowing for the modeling of short-range ordering. This formalism allows for the selection of the composition of maximum short-range ordering through its coordination numbers, corresponding to the minimum of the Gibbs energy that is often found near the composition of the lowest eutectic. By fixing either the cation−cation or anion−anion coordination number, the opposite coordination number is also obtained through eq 3, where $q_i$ is the charge of the respective ions. The coordination


https://doi.org/10.1021/acs.jpcc.4c07788
J. Phys. Chem. C 2025, 129, 2726−2738

Table 2. Thermodynamic Functions Used in the CALPHAD Model in This Work[a]

| compound | $\Delta_f H^\circ_m$ (298) (J mol$^{-1}$) | $S^\circ_m$ (298) (J K$^{-1}$ mol$^{-1}$) | $C_{p,m}(T)$(J K$^{-1}$ mol$^{-1}$) = $a + bT + cT^{-2} + dT + eT^{\frac{1}{2}}$ | | | | | temperature range (K) | source |
|---|---|---|---|---|---|---|---|---|---|
| | | | $a$ | $b$ | $c$ | $d$ | $e$ | | |
| NaCl(s) | −411,260 | 72.15 | 47.72158 | 0.0057 | −882.996 | $1.21466 \times 10^{-5}$ | | [298−1074] | van Oudenaren et al.[19] |
| NaCl(l) | −383,060 | 98.407 | 47.72158 | 0.0057 | −882.996 | $1.21466 \times 10^{-5}$ | | [1074−2500] | Dumaire et al.[21] |
| NaCl(l) | | | 68 | | | | | [1074−2500] | Dumaire et al.[21] |
| NaI(s) | −289,630 | 98.56 | 41.97056 | 0.0251811 | 232,099.4 | $4.761618 \times 10^{-9}$ | | [298−934] | Chase[10] |
| NaI(l) | −271,470 | 112.518439094993 | 67 | | | | | [934−3400] | Chase[10] |
| $MgCl_2$(s) | −641,616 | 89.629 | 54.5843 | 0.0214213 | −1,112,119 | $-2.3567 \times 10^{-6}$ | 399.177 | [298−2000] | Chase[10] |
| $MgCl_2$(l) | −601,680.1 | 129.236 | 193.4089 | −0.3620139 | −3,788,504 | $3.199871 \times 10^{-4}$ | | [298−660] | Chase[10] |
| | | | 92.048 | | | | | [660−2500] | Chase[10] |
| $MgI_2$(s) | −370,000 | 134 | 68.94675 | 0.01854692 | −237.9452 | $1.12469 \times 10^{-8}$ | | [298−906] | Chase[10] |
| $MgI_2$(l) | −344,000 | 162.698 | 68.94675 | 0.01854692 | −237.9452 | $1.12469 \times 10^{-8}$ | | [298−906] | Chase[10] |
| | | | 100 | | | | | [906−2000] | Chase[10] |
| $NaMgCl_3$(s) | **−1,063,200** | **155.5** | 90 | 0.075 | | | | [298−1000] | Chartrand and Pelton,[24] this work |
| $Na_2MgCl_4$(s) | **−1,486,000** | **211** | 135 | 0.1125 | | | | [298−773] | Chartrand and Pelton,[24] this work |
| $Na_6MgCl_8$(s) | **−3,148,000** | **481.5** | 340.9138 | 0.055621 | −1,117,417 | $7.05 \times 10^{-5}$ | 399.177 | [298−6000] | This work |
| $Na_2Mg_3Cl_8$(s) | **−2,766,000** | **410** | 252.3333 | 0.059943 | −2,226,887 | $3.17 \times 10^{-5}$ | 798.354 | [298−6000] | This work |

[a]Optimized values are marked in bold.

numbers used in the thermodynamic model presented in this work are given in Table 3.

$$\frac{q_A}{Z^A_{AB/XY}} + \frac{q_B}{Z^B_{AB/XY}} = \frac{q_X}{Z^X_{AB/XY}} + \frac{q_Y}{Z^Y_{AB/XY}} \tag{3}$$

Table 3. Coordination Numbers Used in the CALPHAD Model Presented in This Work

| A | B | X | Y | $Z^A_{AB/XY}$ | $Z^B_{AB/XY}$ | $Z^X_{AB/XY}$ | $Z^Y_{AB/XY}$ |
|---|---|---|---|---|---|---|---|
| Na | Na | Cl | Cl | 6 | 6 | 6 | 6 |
| Mg | Mg | Cl | Cl | 6 | 6 | 3 | 3 |
| Na | Na | I | I | 6 | 6 | 6 | 6 |
| Mg | Mg | I | I | 6 | 6 | 3 | 3 |
| Na | Mg | Cl | Cl | 3 | 6 | 3 | 3 |
| Na | Mg | I | I | 6 | 6 | 4 | 4 |
| Mg | Mg | Cl | I | 6 | 6 | 3 | 3 |
| Na | Na | Cl | I | 6 | 6 | 6 | 6 |

The excess parameters that are optimized are those related to the second-nearest neighbor exchange reactions as given in eqs 4−6. The associated change in Gibbs energy of eqs 4−6 is expressed in eqs 7−9.

$$(A_2X_2)_{quad} + (B_2X_2)_{quad} \rightarrow 2(ABX_2)_{quad} \quad \Delta g_{AB/XX} \tag{4}$$

$$(A_2X_2)_{quad} + (A_2Y_2)_{quad} \rightarrow 2(A_2XY)_{quad} \quad \Delta g_{AA/XY} \tag{5}$$

$$(ABX_2) + (ABY_2) + (A_2XY) + (B_2XY) \rightarrow 4(ABXY) \quad \Delta g_{AB/XY} \tag{6}$$

$$\Delta g_{AB/XX} = \Delta g^0_{AB/XX} + \Sigma_{i\geq 1} g^{i0}_{AB/XX} \chi^i_{AB/XX} + \Sigma_{j\geq 1} g^{0j}_{AB/XX} \chi^j_{BA/XX} \tag{7}$$

$$\Delta g_{AA/XY} = \Delta g^0_{AA/XY} + \Sigma_{i\geq 1} g^{i0}_{AA/XY} \chi^i_{AA/XY} + \Sigma_{j\geq 1} g^{0j}_{AA/XY} \chi^j_{AA/YX} \tag{8}$$

$$\Delta g_{AB/XY} = \Delta g^0_{AB/XY} + \Sigma_{i\geq 1} (g^i_{AB/XY(AX)} \chi^i_{AA/XX} + g^i_{AB/XY(BX)} \chi^j_{BB/XX} + g^i_{AB/XY(AY)} \chi^j_{AA/YY} + g^i_{AB/XY(BY)} \chi^j_{BB/YY}) \tag{9}$$

In eq 7, the terms $\Delta g^0_{AB/XX}$, $g^{i0}_{AB/XX}$, and $g^{0j}_{AB/XX}$ are composition-independent coefficients that may depend on temperature. The composition dependence of the Gibbs energy is apparent through $\chi_{AB/XX}$ as these are defined as per eq 10. In this equation, $X_{AA}$ is the cation−cation pair fraction or the molar fraction of the quadruplet containing two cations A. For this binary system, $\{X_{AA} + X_{AB} + X_{BB}\}$ is equal to one.

$$\chi_{AB/XX} = \frac{X_{AA}}{X_{AA} + X_{AB} + X_{BB}} \tag{10}$$

The Gibbs energy functions used in this work to describe the liquid solutions are given in eqs 11−14 for the NaCl−$MgCl_2$, NaI−$MgI_2$, NaCl−NaI, and $MgCl_2$−$MgI_2$ systems, respectively. Using the data for the binary systems as a basis, extrapolations to the ternary and quaternary fields were made with Kohler/Toop interpolations, due to the asymmetry of the system. In this work, $MgCl_2$ and $MgI_2$ are considered



https://doi.org/10.1021/acs.jpcc.4c07788
J. Phys. Chem. C 2025, 129, 2726−2738

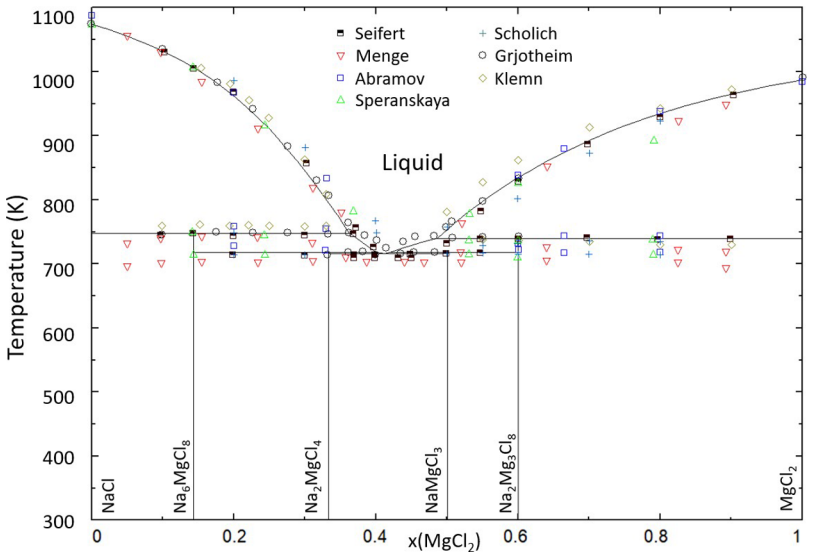


**Figure 1.** Phase diagram of the NaCl−$MgCl_2$ system, calculated with the CALPHAD model presented in this work. Experimental data from Seifert and Fink[27] (black, half-filled squares), Menge[37] (red, open downward triangles), Abramov[35] (blue, open squares), Speranskaya[36] (lime green, upward open triangles), Scholich[30] (azure, crosses), Grjotheim et al.[33] (black, open circles), and Klemn et al.[31] (khaki, open diamonds) are shown for comparison with the calculated phase diagram.

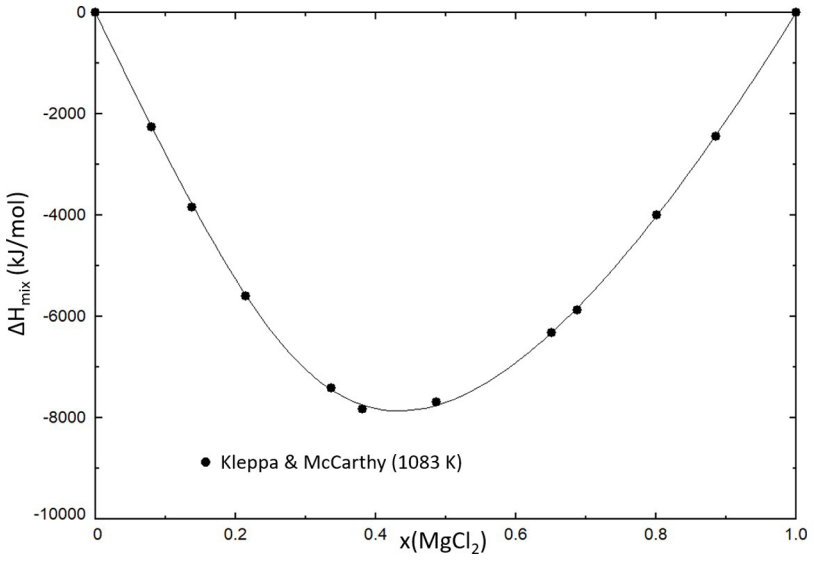


**Figure 2.** Mixing enthalpy of the NaCl−$MgCl_2$ system, calculated at $T$ = 1083 K, compared to experimental data from Kleppa and McCarthy,[38] measured at $T$ = 1083 K.

asymmetric components, as their ionic structure in the liquid (i.e., molecular species) is different from the sodium halides (i.e., ionic species). The ternary and reciprocal interaction parameters needed to optimize the pseudobinaries NaI−$MgCl_2$ and NaCl−$MgI_2$, as well as the quaternary field, are given in eqs 15−17.

$$\Delta g_{NaMg/ClCl} = -10200 - 0.75T + (660.5)\chi_{NaMg/ClCl} + (-4650)\chi_{MgNa/ClCl} \quad (11)$$

$$\Delta g_{NaMg/II} = -5500 + 3.5T + (-3000 - 3.5T)\chi_{NaMg/II} + (500 + 0.2T)\chi_{MgNa/II} + (2T)\chi^2_{NaMg/II} \quad (12)$$

$$\Delta g_{NaNa/ClI} = 550 + 0.5T + (300 + 1.5T)\chi_{NaNa/ICl} \quad (13)$$

$$\Delta g_{MgMg/ClI} = 3000 - T + (-4T)\chi_{MgMg/ClI} + (3000 + 3T)\chi_{MgMg/ICl} + (1500)\chi^2_{MgMg/ClI} + (-1500)\chi^2_{MgMg/ICl} \quad (14)$$

$$\Delta g^0_{NaMg/ClI(NaCl)} = -3000 \quad (15)$$

$$\Delta g^0_{NaMg/ClI(NaI)} = -3000 \quad (16)$$

$$\Delta g^{001}_{NaMg/ClCl(I)} = -3000 \quad (17)$$

*2.2.3. Solid Solution Modeling.* The thermodynamic description of solid solutions is done using the two-sublattice



https://doi.org/10.1021/acs.jpcc.4c07788
J. Phys. Chem. C 2025, 129, 2726−2738

**Table 4. Calculated Invariant Equilibria in the NaCl−$MgCl_2$ System, As Well As Experimentally Measured Values of These Invariants from Seifert and Fink,[27] Grjotheim et al.,[33] Menge,[37] Speranskaya,[36] Scholich,[30] Abramov[35] and Klemm et al.,[31] As Well As the Thermodynamic Assessment of Chartrand and Pelton[24]**

| | modeling ($T$ (K)) | | | experimental data ($T$ (K)) | | | | | | | |
|---|---|---|---|---|---|---|---|---|---|---|---|
| $x(MgCl_2)$ | this work | Chartrand | Grjotheim | Seifert | Menge | Sperenskaya | Scholich | Abramov | Klemm | equilibrium | invariant reaction |
| 0 | 1074 | 1074 | 1073 | | | 1072 | | 1086 | | congruent melting | NaCl = L |
| 0.143 | 744 | 748[a] | 747[a] | 747 | 742[a] | 749[a] | 747[a] | 757[a] | 760[a] | peritectic | $Na_6MgCl_8$ = NaCl + L′ |
| 0.333 | 713 | | | 715 | | | | | | peritectic | $Na_2MgCl_4$ = $Na_6MgCl_8$ + L′ |
| 0.415 | 711 | 732 | 724 | 709 | 702 | 714 | 713 | 721 | | eutectic | $Na_2MgCl_4$ + $NaMgCl_3$ = L |
| 0.5 | 715 | 739 | 740 | 716 | 717 | 735 | 728 | 730 | 734 | peritectic | $NaMgCl_3$ = $Na_2Mg_3Cl_8$ + L′ |
| 0.6 | 736 | | | 740 | | | | | | peritectic | $Na_2Mg_3Cl_8$ = $MgCl_2$ + L′ |
| 1 | 987 | 987 | 991 | | | | | 984 | | congruent melting | $MgCl_2$ = L |

[a]Reported temperatures were interpreted as the peritectic reaction $Na_2MgCl_4$ = NaCl + L′ in the literature.

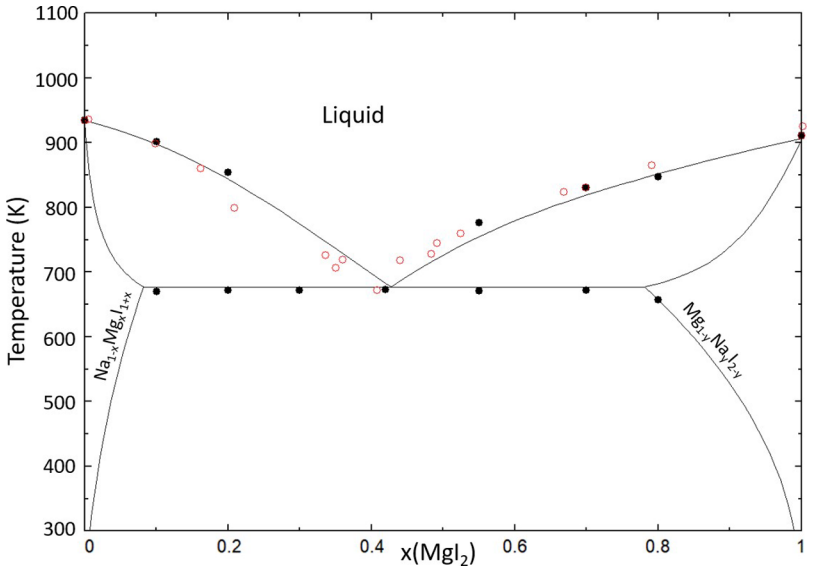


**Figure 3.** Phase diagram of the NaI−$MgI_2$ system as calculated with the CALPHAD model presented in this work. Experimental data from Klemn et al.[31] (red, open circles) and this work (black, closed circles).

polynomial model to be consistent with the description of the JRC Molten Salt Database (JRCMSD).[26] The Gibbs Energy function of the solid-solution is given in eq 18.

$$G(T) = X_A \cdot G_A^0 + X_B \cdot G_B^0 + X_A RT \ln X_A + X_B RT \ln X_B + \Delta G_m^{excess} \quad (18)$$

In the above equation, $G_i^0$ are the end-member molar Gibbs energies, and $X_i$ are the site molar fractions of the end-members A and B, respectively. The third and fourth terms in eq 18 represent the configurational entropy. The excess Gibbs energy, present in eq 18 as $\Delta G_m^{excess}$, is defined as per eq 19.

$$\Delta G_m^{excess} = \Sigma_{i,j \geq 1} y_A^i y_B^i L_{AB}^{ij} \quad (19)$$

The term $L_{AB}^{ij}$ in eq 19 is an interaction coefficient that can be a function of temperature if necessary. The equivalent site fractions $y_A$ and $y_B$ are charge equivalent site fractions defined as in eq 20, where the term $q^i$ is the charge of species $i$.

$$y_A = \frac{q^A X_A}{q^A X_A + q^B X_B} \quad (20)$$

The Gibbs energy function of the solid solution in the NaCl−NaI system is given in eq 21 The Gibbs energy function used in this work to describe the mutual solid solubility of the end-members in the NaI−$MgI_2$ system is given in eq 22. For the solid solution in the $MgCl_2$−$MgI_2$ system, the associated Gibbs energy function is given in eq 23.

$$\Delta G_{m,ICl}^{excess} = y_I y_{Cl}(30{,}000 - 5T) \quad (21)$$

$$\Delta G_{m,NaMg}^{excess} = y_{Na} y_{Mg}(-1000) + y_{Na} y_{Mg}^2(14{,}000) + y_{Na}^2 y_{Mg}(9000) \quad (22)$$

$$\Delta G_{m,ICl}^{excess} = y_I y_{Cl}(-1000 + 6.5T) + y_I y_{Cl}^2(20{,}000) + y_I^2 y_{Cl}(10T) \quad (23)$$



https://doi.org/10.1021/acs.jpcc.4c07788
J. Phys. Chem. C 2025, 129, 2726−2738

## 3. RESULTS AND DISCUSSION

**3.1. NaCl−$MgCl_2$.** Four intermediates in the NaCl−$MgCl_2$ system have been identified in the literature, and their crystallographic information has been reported by Seifert and Fink,[27] van Loon and IJdo,[28] and Kanno et al.[29] These intermediates are $NaMgCl_3$ (SGR $R\ \bar{3}h$), $Na_2MgCl_4$ (SGR $Pbam$), $Na_6MgCl_8$ (SGR $Fm\ \bar{3}m$), and $Na_2Mg_3Cl_8$ (SGR $R\ \bar{3}mh$).

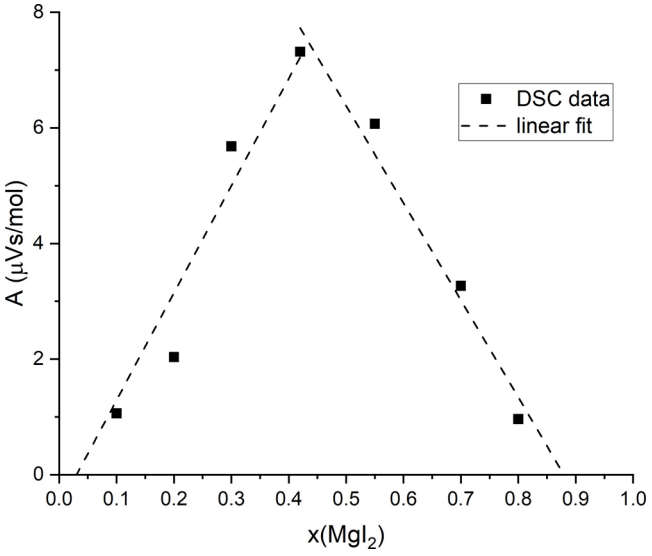


**Figure 4.** Tammann diagram of the NaI−$MgI_2$ system, calculated using the areas of the eutectic equilibria measured in this work by DSC.

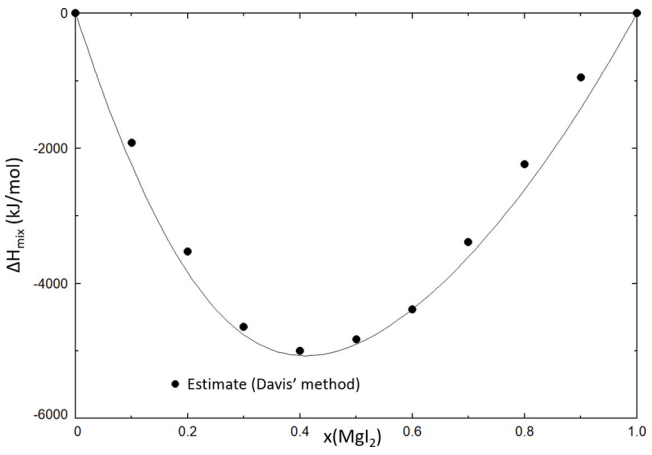


**Figure 5.** Mixing enthalpy of the NaI−$MgI_2$ system, calculated at $T$ = 1000 K, compared to the estimated mixing enthalpy obtain using the estimation method of Davis and Rice.[8]

The invariant equilibria in the NaCl−$MgCl_2$ system have been investigated abundantly in the literature[30−37] and a CALPHAD model using the quadruplet approximation in the quasichemical formalism has been presented by Chartrand and Pelton[24] based on the data in the literature. However, in the model by Chartrand et al., the intermediate $Na_2MgCl_4$ is unstable at room temperature, which is not consistent with the corresponding crystallographic literature.[27−29] Furthermore, the assessment by Chartrand and Pelton[24] does not include the intermediates $Na_6MgCl_8$ and $Na_2Mg_3Cl_8$, of which crystal structures have been reported in the literature.[27,28] In this work, we have identified the intermediate $Na_6MgCl_8$ from XRD measurements in the quaternary system. For these reasons, the NaCl−$MgCl_2$ system is reassessed in this work.

The optimized phase diagram of the NaCl−$MgCl_2$ system is presented in Figure 1. The thermodynamic model is in good agreement with most of the available experimental data. An exception is the data from Menge,[37] who measured a single eutectic equilibrium across the entire composition range using thermal analysis on their cooling curves. However, Menge et al. also report a contamination of their $MgCl_2$ with up to 7% MgO, which could explain their results. Moreover, several authors report a double event at $x(MgCl_2) \geq 0.6$ between 700 and 750 K, which is in contrast with what our model predicts. However, since the most recent publications, those being the work of Grjotheim et al.[33] and Seifert and Fink[27] do not measure this double event, we decided to follow Seifert's assessment of this section of the phase diagram.

The thermodynamic model was moreover optimized to fit the experimental mixing enthalpy data. The calculated mixing enthalpy of this system is given in Figure 2, and is compared to the experimental data from Kleppa and McCarthy,[38] who measured the mixing enthalpy at 1083 K using the break-off ampule method.

A comparison between the invariant equilibria presented in the literature, and those calculated with the thermodynamic model is given in Table 4. The CALPHAD model is in good agreement with the experimental data for the melting points of the end members, as well as the eutectic temperature. There is a slight deviation from most literature in the peritectic equilibria of $Na_2MgCl_4$ and $NaMgCl_3$, which are modeled lower than reported. This is due to the fact that the peritectic equilibria of $Na_2MgCl_4$ and $NaMgCl_3$ in the literature, are interpreted here as the peritectics of $Na_6MgCl_8$ and $Na_2Mg_3Cl_8$ in accordance with Seifert and Fink.[27]

**3.2. NaI−$MgI_2$.** The system NaI−$MgI_2$ has been investigated previously by Klemn et al.,[31] and in this work, we have aimed to complement that data. The experimental data on invariant equilibria obtained in this work is given in the Supporting Information in Table S4. Seifert et al. assumed the existence of a eutectic system with wide solid solutions at both end-members, which seems to be disproven by our data, as evidenced by the eutectic event that is measured at

**Table 5. Calculated Invariant Equilibria in the NaI−$MgI_2$ System Compared to Experimentally Measured Values in This Work Using DSC, as Well as the Data from Klemn et al.[31]**

| | $T$ (K) | | | | |
|---|---|---|---|---|---|
| $x(MgCl_2)$ | CALPHAD | this work (DSC) | Klemn | equilibrium | invariant reaction |
| 0 | 933 | 934 ± 5 | 932 | congruent melting | NaI = L |
| 0.4 | 671 | 665 ± 10 | 669 | eutectic | $Na_{1-x}Mg_xCl_{1+x} + Na_yMg_{1-y}Cl_{2-y}$ = L |
| 1 | 905 | 911 ± 5 | 909 | congruent melting | $MgI_2$ = L |



https://doi.org/10.1021/acs.jpcc.4c07788
J. Phys. Chem. C 2025, 129, 2726−2738

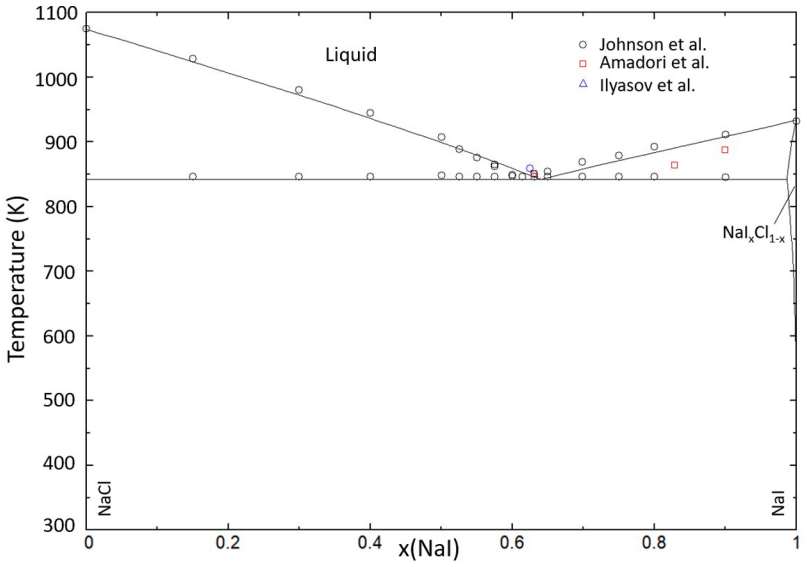


**Figure 6.** Phase diagram of the NaCl−NaI system calculated with the thermodynamic model presented in this work. Experimental data from Johnson and Hathaway[39] (black, open circles), Amadori[40] (red, open squares), and Ilyasov et al. (blue, open triangle) are compared to the calculated phase equilibria.

**Table 6. Calculated Invariant Equilibria in the NaCl−NaI System Compared to Experimentally Measured Values from Johnson and Hathaway,[39] Amadori,[40] and Ilyasov and Bostandzhiyan[45]**

| | $T$ (K) | | | | | |
|---|---|---|---|---|---|---|
| $x$(NaI) | CALPHAD | Johnson | Amadori | Ilyasov | equilibrium | invariant reaction |
| 0 | 1074 | 1073 | | | congruent melting | NaCl = L |
| 0.622 | 848 | 845 | 850 | 858 | eutectic | NaCl + NaI = L |
| 1 | 933 | 931 | | | congruent melting | NaI = L |

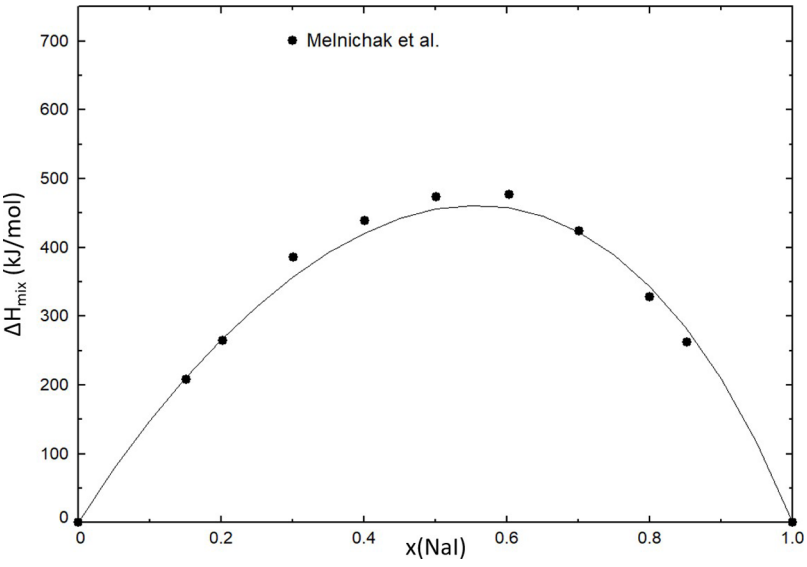


**Figure 7.** Mixing enthalpy of the NaCl−NaI system, calculated at 1084 K, compared to the experimental data from Melnichak and Kleppa[44] obtained at 1084 K.

compositions $0.1 \leq x(MgI_2) \leq 0.7$. Based on the measured eutectic events, a Tammann diagram was drawn up that corroborates the eutectic composition and the existence of a mutual solid solution. The optimized phase diagram is shown in Figure 3, and the Tammann diagram is given in Figure 4.

The Tammann diagram shown in Figure 4 shows that the composition of the eutectic is $x(MgI_2) = 0.40$, and the limits of the solid solution are approximately $x(MgI_2) = 0.07$ and 0.87, respectively. This is in good agreement with the thermodynamic model. The calculated mixing enthalpy of this system is shown in Figure 5. No data were available in the literature for the mixing enthalpy of the liquid in this system. To obtain an estimate of the mixing enthalpy to which the model could be fit, the empirical method of Davis and Rice[8] was used. This method is based on the size difference between the cations in a molten salt system, as discussed in the work of Alders et al.[9]



https://doi.org/10.1021/acs.jpcc.4c07788
J. Phys. Chem. C 2025, 129, 2726−2738

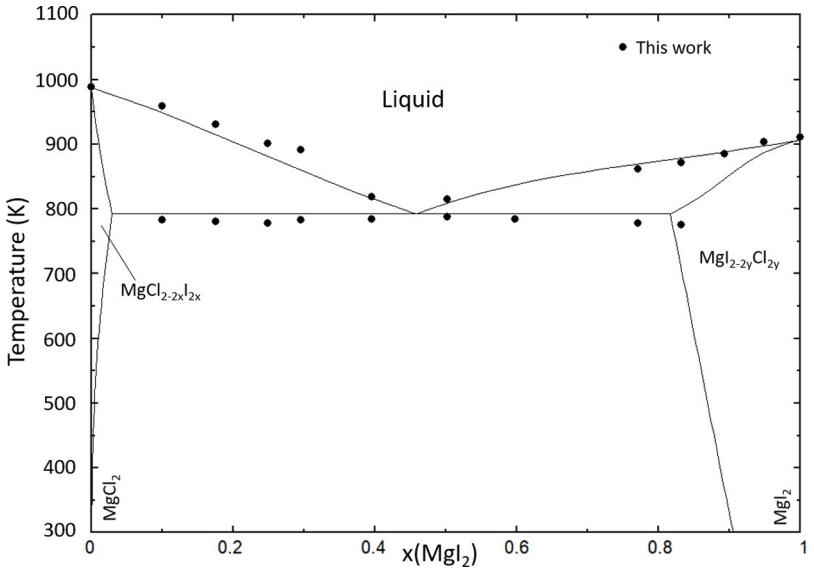


**Figure 8.** Phase diagram of the $MgCl_2$−$MgI_2$ system calculated with the thermodynamic model presented in this work. Experimental data obtained in this work (black circles) are compared to the calculated equilibria.

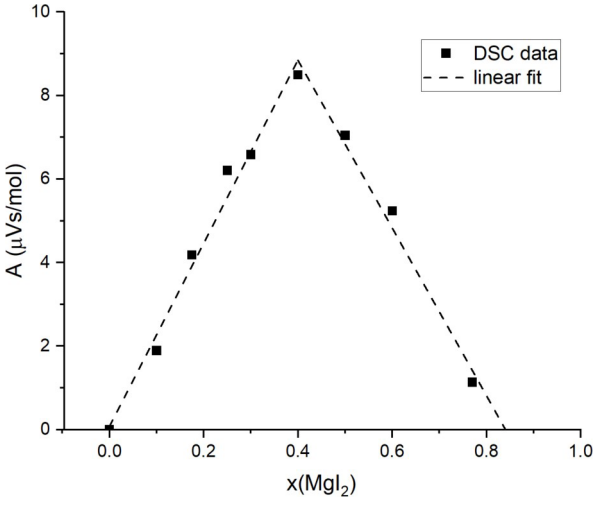


**Figure 9.** Tammann diagram of the $MgCl_2$−$MgI_2$ system, calculated using the area of the eutectic equilibria measured in this work by DSC (black circles).

The invariant equilibria measured in this work are compared to the data from Klemn et al.[31] and the thermodynamic model in Table 5.

**3.3. NaCl−NaI.** The full system NaCl−NaI has been previously investigated experimentally by Johnson and Hathaway.[39] The eutectic has been measured as well by Amadori[40] and Ilyasov and Bergman,[41] at a slightly different composition and temperature. Furthermore, Amadori et al. report solidus data at $x(NaI) = 0.83$ and 0.9, which they attributed to the formation of a solid solution. Johnson et al. did not find any evidence of solid solubility between NaCl and NaI in their XRD and thermal analyses, however. Oonk et al.[42,43] suggest that negligible solid solubility in the Na(Cl,I) system can be expected based on the crystal sizes, so for this reason, solid solubility has been included in the thermodynamic model shown in Figure 6. Table 6 shows the comparison between the invariant equilibria calculated with the thermodynamic model and those reported in the literature. This table shows good agreement with the eutectic equilibria reported in the literature.

The mixing enthalpy of this system has been measured experimentally by Melnichak and Kleppa.[44] The CALPHAD model presented in this work has been optimized to fit the mixing enthalpy, and the agreement between the model and the experimental data is shown in Figure 7.

**3.4. $MgCl_2$−$MgI_2$.** The system $MgCl_2$−$MgI_2$ has been investigated experimentally for the first time in this work, and a CALPHAD model of this system has been constructed, as shown in Figure 8. The invariant equilibria measured experimentally by DSC are given in the Supporting Information in Table S1. A Tammann diagram of this system is presented in Figure 9. The Tammann diagram, as well as the absence of the eutectic event at compositions $x(MgI_2) \geq 0.85$, indicate that a solid solution in the $MgI_2$-rich region of the phase diagram is stable, with the composition $MgI_{2-2y}Cl_{2y}$.

**Table 7. Calculated Invariant Equilibria in the $MgCl_2$−$MgI_2$ System Compared to Experimentally Measured Values from Johnson and Hathaway,[39] Amadori,[40] and Ilyasov and Bostandzhiyan[45]**

| | $T$ (K) | | | |
|---|---|---|---|---|
| $x(MgI_2)$ | CALPHAD | this work (DSC) | equilibrium | invariant reaction |
| 0 | 987 | 988 ± 5 | congruent melting | $MgCl_2 = L$ |
| 0.452 | 786 | 784[a] ± 10 | eutectic | $MgCl_{2-2x}I_{2x} + MgI_{2-2y}Cl_{2y} = L$ |
| 1 | 905 | 911 ± 5 | congruent melting | $MgI_2 = L$ |

[a]The average value of measured eutectic equilibria is shown in Figure 8.



https://doi.org/10.1021/acs.jpcc.4c07788
J. Phys. Chem. C 2025, 129, 2726−2738

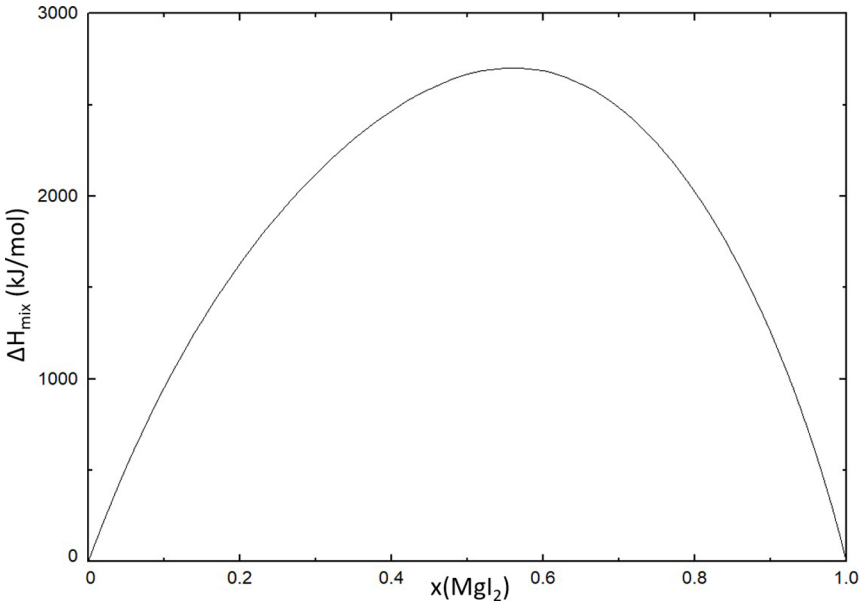


**Figure 10.** Mixing enthalpy of the $MgCl_2$−$MgI_2$ system calculated using the CALPHAD method presented in this work.

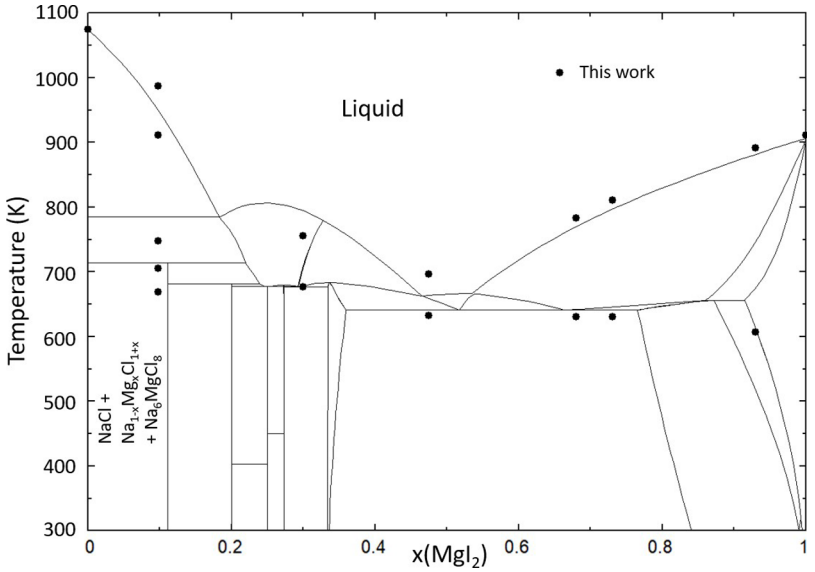


**Figure 11.** Phase diagram of the system NaCl−$MgI_2$ calculated with the optimized quaternary model presented in this work. Experimental data obtained in this work (black circles). The labeled phase fields correspond to phase fields where post-DSC XRD measurements have been performed.

Moreover, the invariant equilibria measured in this work, and those calculated with the thermodynamic model, are shown in Table 7.

There is no experimental data on the mixing enthalpy of the $MgCl_2$−$MgI_2$ system available in the literature. Furthermore, no experimental data on similar systems $MCl_2$−$MI_2$ is known either, to the best of our knowledge, which makes estimating the mixing enthalpy using Davis' method impossible. The calculated enthalpy of mixing obtained using the CALPHAD model presented in this work is given in Figure 10. This figure shows a positive deviation from ideality, which is also observed for the mixed chloride-iodide systems with alkali metals[44] (ACl−AI, A = Li, Na, K, Rb, and Cs).

**3.5. NaCl−$MgI_2$ and NaI−$MgCl_2$.** In order to assess the accuracy of the thermodynamic model, an experimental investigation of the quaternary system NaCl−NaI−$MgCl_2$−$MgI_2$ has been performed of the systems along the quaternary diagonals NaCl−$MgI_2$ and NaI−$MgCl_2$. The investigation of these pseudobinary systems is discussed in Sections 3.5.1 and 3.5.2, respectively.

*3.5.1. NaCl−$MgI_2$.* The NaCl−$MgI_2$ binary system has been investigated using DSC and XRD. The DSC measurements of the invariant equilibria are shown in the Supporting Information in Table S2 and on the phase diagram in Figure 11. In order to improve the agreement between the extrapolated phase diagram of the NaCl−$MgI_2$ system and the experimental data, reciprocal terms were added to the CALPHAD model as listed in Section 2.2.2. The CALPHAD model describes the measured invariant equilibria well, though there are discrepancies at $x(MgI_2) = 0.098$, which can be due to some currently unexplained subsolidus behavior.



https://doi.org/10.1021/acs.jpcc.4c07788
J. Phys. Chem. C 2025, 129, 2726−2738

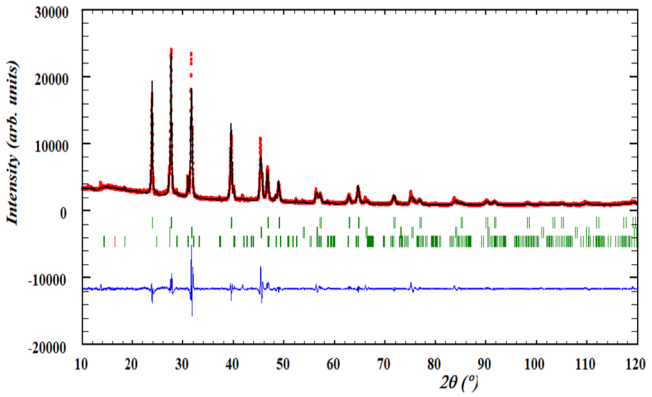


**Figure 12.** Profile refinement of the XRD obtained from the post-DSC sample at $x(MgI_2) = 0.1$ in the NaCl−$MgI_2$ system. Phases used in the refinement are NaCl, NaI, $NaMgCl_3$, and $Na_6MgCl_8$. The observerd intensity (red circles) is shown alongside the calculated intensity (black line), and the difference between the two is shown (blue line). The angles at which reflections occur, i.e., the bragg positions, are shown as well (green, vertical lines).

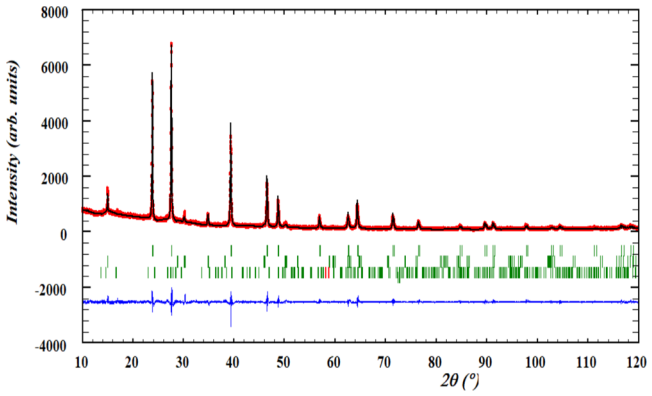


**Figure 14.** Profile refinement of the XRD obtained from the post-DSC sample at $x(MgCl_2) = 0.3$ in the NaI−$MgCl_2$ system. Phases used in the refinement are $MgCl_2$, NaI and $Na_3Mg_2Cl_8$. The observerd intensity (red circles) is shown alongside the calculated intensity (black line), and the difference between the two is shown (blue line). The angles at which reflections occur, i.e., the bragg positions, are shown as well (green, vertical lines).

XRD measurements have been performed on the post-DSC samples at composition $x(MgI_2) = 0.1$, and a profile refinement has been performed using the method of Rietveld, Loopstra, and van Laar.[11,12] The refinement of the sample at $x(MgI_2) = 0.1$ is shown in Figure 12. The phases found with this refinement are NaCl (36.69 wt %), NaI (29.02 wt %), $NaMgCl_3$ (7.21 wt%) and $Na_6MgCl_8$ (27.08 wt %). The expected phases at equilibrium from the thermodynamic model are NaCl, NaI, and $Na_6MgCl_8$. While a sample at full thermodynamic equilibrium should consist of only three phases, it could be that the formation kinetics of these phases were not favorable during cooling in the DSC experiment. This could be the case here, given that the presence of $NaMgCl_3$ in the sample is minor. This experiment also shows that iodine prefers associating with Na over Mg, as evidenced by the fact that NaI is present in the final sample.

*3.5.2. NaI−$MgCl_2$.* The NaI−$MgCl_2$ binary system has also been investigated using DSC and XRD. The DSC measurements of the invariant equilibria are shown in the Supporting Information in Table S3 and on the phase diagram in Figure 13. In order to improve the agreement between the extrapolated phase diagram of the NaI−$MgCl_2$ system and the experimental data, reciprocal terms were added to the CALPHAD model as listed in Section 2.2.2. The model agrees well with the measured invariant equilibria, with the exception of two points at $x(MgCl_2) = 0.2$, around $T = 630$ K. These measured equilibria could be due to some currently unexplained subsolidus behavior.

Post-DSC XRD analysis of some samples in the NaI−$MgCl_2$ system has been performed in order to investigate how well the thermodynamic model predicts the stable solid phases. The refinement of the DSC sample taken at $x(MgCl_2) = 0.3$ is shown in Figure 14. The refinement shows that the dominant

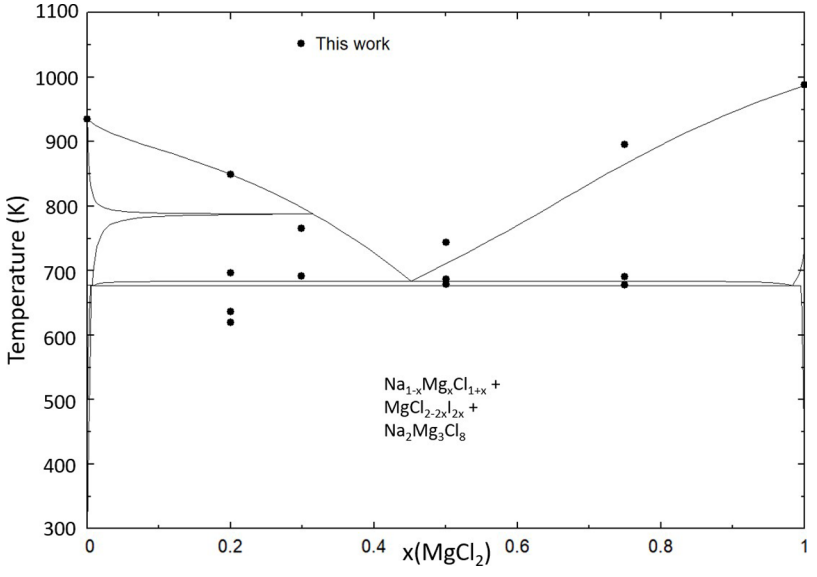


**Figure 13.** Phase diagram of the system NaI−$MgCl_2$ calculated with the optimized quaternary model presented in this work. Experimental data obtained in this work (black circles). The labeled phase field corresponds to the phase field where post-DSC XRD measurements have been performed.



https://doi.org/10.1021/acs.jpcc.4c07788
J. Phys. Chem. C 2025, 129, 2726−2738

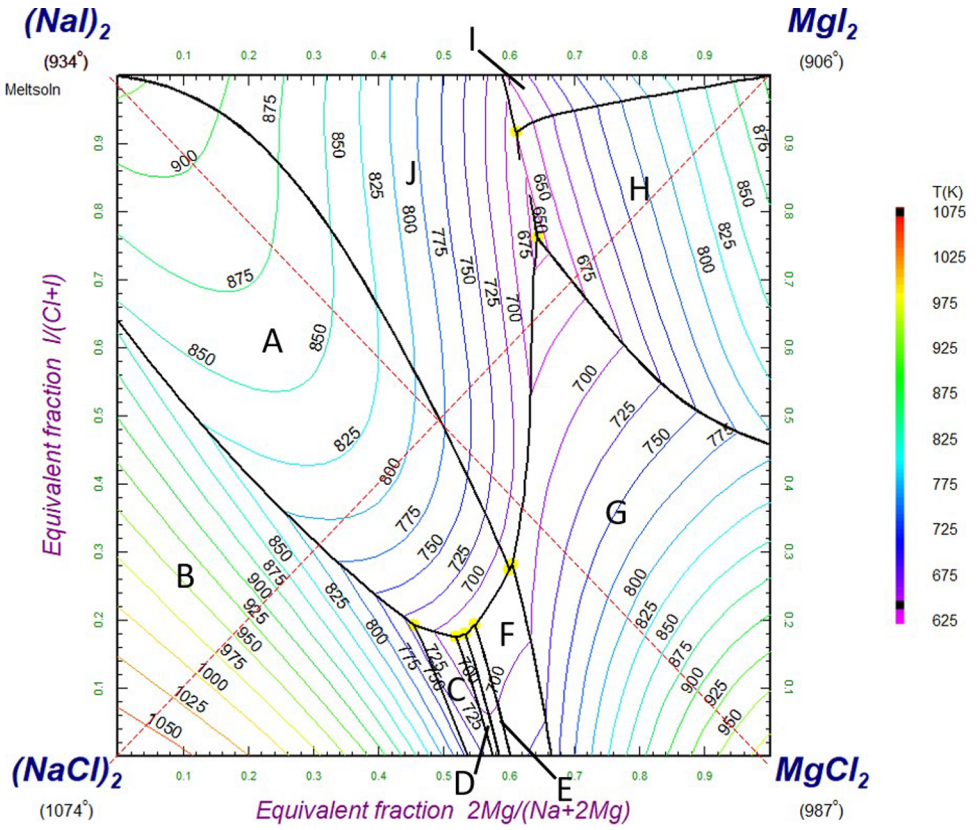


**Figure 15.** Liquidus projection of the Na−Mg−Cl-I quaternary system. Primary crystallization phases labeled A-I are $Na_{1-x}I_xCl_{1-x}$ (A), NaCl (B), $Na_6MgCl_8$ (C), $Na_2MgCl_4$ (D), $NaMgCl_3$ (E), $Na_2Mg_3Cl_8$ (F), $MgI_{2-2x}Cl_{2x}$ (G), $MgCl_{2-2y}I_{2y}$ (H), $Na_yMg_{1-y}Cl_{2-y}$ (I), $Na_{1-x}Mg_xCl_{1+x}$ (J). Dashed red lines indicate the pseudobinary sections $NaCl-MgI_2$ and $NaI-MgCl_2$, also shown in Figures 11 and 13 respectively.

**Table 8. Calculated Invariant Equilibria in the $NaCl-NaI-MgCl_2-MgI_2$ System**

| fraction 2Mg/(Na + 2Mg) | fraction I/(Cl + I) | $T$ (K) | invariant reaction |
|---|---|---|---|
| 0.45 | 0.19 | 713 | NaCl, $Na_6MgCl_8$, $Na_{1-x}Mg_xI_{1+x}$ |
| 0.52 | 0.17 | 681 | $Na_2MgCl_4$, $Na_6MgCl_8$, $Na_{1-x}Mg_xI_{1+x}$ |
| 0.60 | 0.27 | 677 | $MgI_{2-2y}Cl_{2y}$, $Na_2Mg_3Cl_8$, $Na_{1-x}Mg_xI_{1+x}$ |
| 0.55 | 0.19 | 677 | $Na_2Mg_3Cl_8$, NaMgCl, $Na_{1-x}Mg_xI_{1+x}$ |
| 0.53 | 0.18 | 677 | $Na_2MgCl_4$, $NaMgCl_3$, $Na_{1-x}Mg_xI_{1+x}$ |
| 0.61 | 0.91 | 677 | $MgI_{2-2y}Cl_{2y}$, $MgCl_{2-2x}I_{2x}$, $Na_{1-x}Mg_xI_{1+x}$ |
| 0.64 | 0.77 | 641 | $MgI_{2-2y}Cl_{2y}$, $Mg_{1-y}Na_yI_{2-y}$, $Na_{1-x}Mg_xI_{1+x}$ |

phases at this composition are $Na_{1-x}Mg_xI_{1+x}$ and $MgCl_2$, which is in agreement with the thermodynamic model predictions. In the thermodynamic model, $Na_2Mg_3Cl_8$ is also predicted to be stable at room temperature, however only at a concentration of $1.05 \times 10^{-5}$ mole per mole $NaI-MgCl_2$ mixture. This is expected to be below the detection limit of this XRD; hence, it explains that it is not measured here. Additionally, in the Supporting Information in Figure S1, the profile refinement of composition $x(MgCl_2) = 0.75$ is shown.

*3.5.3. Quaternary Liquidus Projection.* The liquidus projection of this quaternary system is presented in Figure 15. The optimization of this quaternary system was done based on the pseudobinary systems $NaCl-MgI_2$ and $NaI-MgCl_2$, as detailed in Sections 3.5.1 and 3.5.2. The calculated invariant equilibria in the quaternary system are shown in Table 8.

## 4. SUMMARY

A thermodynamic model of the quaternary fused salt system $NaCl-NaI-MgCl_2-MgI_2$ has been presented in this work using the CALPHAD method with the quasi-chemical formalism in the quadruplet approximation for the liquid solution. Two of the binary subsystems of this quaternary system have been reoptimized based on data from the literature. The first system is NaCl−NaI, which has been assessed as a simple binary eutectic. In contrast to previous assessments, no solid solubility has been included in this model. Second is the $NaCl-MgCl_2$ system, which was reoptimized to include four intermediates: $NaMgCl_3$, $Na_2MgCl_4$, $Na_2Mg_3Cl_8$, and $Na_6MgCl_8$. Contrary to previous assessments of this system,[24,30,31,33,35−37] in which only two of the aforementioned intermediates were included, we retain the assessment of Seifert and Fink,[27] supported by the fact that we have observed $Na_6MgCl_8$ with XRD in a mixture.


https://doi.org/10.1021/acs.jpcc.4c07788
J. Phys. Chem. C 2025, 129, 2726−2738

The $MgCl_2$−$MgI_2$ system has been investigated experimentally for the first time in this work. This system is characterized by (i) a single eutectic at $x(MgI_2) = 0.43$ and $T = 790 \pm 10$ K, (ii) a solid solution $MgCl_{2-2x}I_{2x}$ (rhombohedral) in the composition range $x(MgI_2) \leq 0.1$, (iii) a solid solution $MgI_{2-2y}Cl_{2y}$ (rhombohedral) in the composition range $x(MgI_2) \geq 0.85$. Additionally, the system NaI−$MgI_2$ has been reassessed based on our own experimental data in addition to the data from the literature. We have shown with our measurements of invariant equilibria that the solubility ranges of NaI in $MgI_2$ and vice versa are much narrower than previously assumed. Furthermore, using a Tammann diagram we have determined the composition of the eutectic and optimized our thermodynamic model accordingly.

Moreover, the pseudobinary systems NaCl−$MgI_2$ and NaI−$MgCl_2$ have been investigated experimentally for the first time. Based on the DSC measurements, the quaternary system was optimized further. Post-DSC XRD measurements were performed to investigate the accuracy of the model predictions on the solid phase, and the obtained experimental results were in agreement with the thermodynamic model.

## ■ ASSOCIATED CONTENT

### Supporting Information

The Supporting Information is available free of charge at https://pubs.acs.org/doi/10.1021/acs.jpcc.4c07788.

Experimental investigation and thermodynamic modeling assessment of the NaCl−NaI−$MgCl_2$−$MgI_2$ quaternary system; experimental DSC data as measured in this work, as well as the profile refinement of the sample at composition $x(MgCl_2) = 0.75$ in the NaI−$MgCl_2$ pseudobinary system (PDF)

## ■ AUTHOR INFORMATION


### Corresponding Author

**Anna L. Smith** − *Reactor Physics and Nuclear Materials, Radiation Science & Technology Department, Faculty of Applied Sciences, Delft University of Technology, 2629JB Delft, The Netherlands;* orcid.org/0000-0002-0355-5859; Email: a.l.smith@tudelft.nl

### Authors

**Dennis C. Alders** − *Reactor Physics and Nuclear Materials, Radiation Science & Technology Department, Faculty of Applied Sciences, Delft University of Technology, 2629JB Delft, The Netherlands;* orcid.org/0009-0004-2206-8329

**Bas A.S. Rooijakkers** − *Reactor Physics and Nuclear Materials, Radiation Science & Technology Department, Faculty of Applied Sciences, Delft University of Technology, 2629JB Delft, The Netherlands*

**Rudy J.M. Konings** − *Reactor Physics and Nuclear Materials, Radiation Science & Technology Department, Faculty of Applied Sciences, Delft University of Technology, 2629JB Delft, The Netherlands*

Complete contact information is available at: https://pubs.acs.org/10.1021/acs.jpcc.4c07788


### Notes

The authors declare no competing financial interest.

## ■ ACKNOWLEDGMENTS

The authors of this paper gratefully acknowledge financial support from the ORANO group, as well as fruitful discussions with Dr. Elisa Capelli.

## ■ REFERENCES


(1) Bettis, E.; Schroeder, R.; Cristy, G.; Savage, H.; Affel, R.; Hemphill, L. The aircraft reactor experiment—design and construction. *Nuclear Science and Engineering* **1957**, *2*, 804−825.

(2) Mcmurray, J. W.; Johnson, K.; Agca, C.; Betzler, B. R.; Kropaczek, D. J.; Besmann, T. M.; Andersson, D.; Ezell, N. *Roadmap for thermal property measurements of Molten Salt Reactor systems (Technical Report ORNL/SPR-2020/1865)*; 2021; 4−22.

(3) Mascaron, M.; Le Meute, T.; Martinet, J.; Pascal, V.; Bertrand, F.; Merle, E. Study of the ARAMIS molten salt reactor behavior during unprotected transients. *ICAPP 2023−2023 International Congress on Advances in Nuclear Power Plants, in conjunction with 38th Korea Atomic Power Annual Conference (ICAPP 2023/KAP Conference)*, 2023; 2023200.

(4) Tiwari, V.; Abbink, T.; Flores, J. O.; Flèche, J.; Gueneau, C.; Chatain, S.; Smith, A.; Martinet, J.; Venard, C. Thermodynamic Assessment of the NaCl-CrCl2, NaCl-CrCl3, and FeCl2-CrCl2 Pseudo-Binary Systems for Describing the Corrosion Chemistry Between Molten Salt Fuel and Steel. *Nuclear Science and Engineering* **2023**, *197*, 3035−3057.

(5) Campbell, D.; Malinauskas, A.; Stratton, W. The chemical behavior of fission product iodine in light water reactor accidents. *Nucl. Technol.* **1981**, *53*, 111−119.

(6) Capelli, E.; Beneš, O.; Konings, R. Thermodynamics of soluble fission products cesium and iodine in the Molten Salt Reactor. *J. Nucl. Mater.* **2018**, *501*, 238−252.

(7) Beneš, O.; Capelli, E.; Morelová, N.; Colle, J.-Y.; Tosolin, A.; Wiss, T.; Cremer, B.; Konings, R. Cesium and iodine release from fluoride-based molten salt reactor fuel. *Phys. Chem. Chem. Phys.* **2021**, *23*, 9512−9523.

(8) Davis, H. T.; Rice, S. A. Perturbation theory of the heats of mixing of fused salts. *J. Chem. Phys.* **1964**, *41*, 14−24.

(9) Alders, D.C.; Vlieland, J.; Thijs, M.; Konings, R.J.M.; Smith, A.L. Experimental investigation and thermodynamic assessment of the BaCl2-CeCl3 system. *Journal of Molecular Liquids* **2024**, *396*, 123997.

(10) Chase, M. W., Jr NIST-JANAF thermochemical tables. *J. Phys. Chem. Ref. Data, Monograph* **1998**, *9*, 1−1951.

(11) Rietveld, H. M. A profile refinement method for nuclear and magnetic structures. *Journal of applied Crystallography* **1969**, *2*, 65−71.

(12) van Laar, B.; Schenk, H. The development of powder profile refinement at the Reactor Centre Netherlands at Petten. *Acta Crystallographica Section A: Foundations and Advances* **2018**, *74*, 88−92.

(13) Rodríguez-Carvajal, J. Recent advances in magnetic structure determination by neutron powder diffraction. *Physica B: Condensed Matter* **1993**, *192*, 55−69.

(14) Beneš, O.; Konings, R. J. M.; Wurzer, S.; Sierig, M.; Dockendorf, A. A DSC study of the $NaNO_3$-$KNO_3$ system using an innovative encapsulation technique. *Thermochim. Acta* **2010**, *509*, 62−66.

(15) Höhne, G.; Cammenga, H.; Eysel, W.; Gmelin, E.; Hemminger, W. The temperature calibration of scanning calorimeters. *Thermochim. Acta* **1990**, *160*, 1−12.

(16) Della Gatta, G.; Richardson, M. J.; Sarge, S. M.; Stølen, S. Standards, calibration, and guidelines in microcalorimetry. Part 2. Calibration standards for differential scanning calorimetry∗(IUPAC Technical Report). *Pure Appl. Chem.* **2006**, *78*, 1455−1476.

(17) Lukas, H. L.; Fries, S. G.; Sundman, B. *Computational Thermodynamics: the Calphad method*; Cambridge University Press, 2007; *131*.

(18) *Centre for Research in Computational Thermochemistry, FactSage 7.2 [computer software]*. http://www.factsage.com.

(19) van Oudenaren, G.; Ocadiz-Flores, J. A.; Smith, A. L. Coupled structural-thermodynamic modelling of the molten salt system NaCl-$UCl_3$. *J. Mol. Liq.* **2021**, *342*, No. 117470.
(20) Alders, D. C.; Cette, D. J.; Konings, R. J. M.; Smith, A. L. Experimental investigation and thermodynamic assessment of the AECl2 NdCl3 (AE = Sr, Ba) systems. *Physical Chemistry, Chemical Physics* **2024**, *26*, 24041−24057.
(21) Dumaire, T.; Ocádiz-Flores, J. A.; Konings, R. J. M.; Smith, A. L. A promising fuel for fast neutron spectrum Molten Salt Reactor: NaCl-$ThCl_4$-$PuCl_3$. *Calphad* **2022**, *79*, No. 102496.
(22) Flores, J. O.; Konings, R.; Smith, A. Using the Quasi-chemical formalism beyond the phase Diagram: Density and viscosity models for molten salt fuel systems. *J. Nucl. Mater.* **2022**, *561*, No. 153536.
(23) Ocádiz Flores, J. A.; Rooijakkers, B. A.; Konings, R. J.; Smith, A. L. Thermodynamic Description of the ACl-ThCl4 (A= Li, Na, K) Systems. *Thermo* **2021**, *1*, 122−133.
(24) Chartrand, P.; Pelton, A. D. Thermodynamic evaluation and optimization of the LiCl-NaCl-KCl-RbCl-CsCl-$MgCl_2$-$CaCl_2$-$SrCl_2$-$BaCl_2$ system using the modified quasichemical model. *Can. Metall. Q.* **2001**, *40*, 13−32.
(25) Pelton, A. D.; Chartrand, P.; Eriksson, G. The modified quasi-chemical model: Part IV. Two-sublattice quadruplet approximation. *Metallurgical and Materials Transactions A* **2001**, *32*, 1409−1416.
(26) Beneš, O. *Thermodynamic database on molten salt reactor systems (Technical Report)*; 2021.
(27) Seifert, H.; Fink, H. Die Struktur des $RbMgCl_3$ und die kristallchemischen Beziehungen zwischen Doppelchloriden des Magnesium und Mangan. *Rev. Chim. Miner.* **1975**, *12*, 466−475.
(28) van Loon, C.; IJdo, D. The crystal structure of $Na_6MnCl_8$ and $Na_2Mn_3Cl_8$ and some isostructural compounds. *Acta Crystallogr. Sect. B: Struct. Crystallogr. Cryst. Chem.* **1975**, *31*, 770−773.
(29) Kanno, R.; Takeda, Y.; Murata, K.; Yamamoto, O. Crystal structure of double chlorides, $Na_2MCl_4$ (M= Mg, Cr, Cd): Correlation with ionic conductivity. *Solid State Ionics* **1990**, *39*, 233−244.
(30) Scholich, K. Ternare Systeme aus Kaliumchlorid, Natrium-chlorid und den Chloriden zweitiger Metalle (L). *Neues Jahrb. Mineral. Geol.* **1920**, *43*, 251−294.
(31) Klemn, W.; Beyersdorfer, K.; Oryschkewitsch, J. Über binäre Systeme aus Halogeniden II): Das Verhalten von NaCl, KCl, RbCl, NaJ und KJ zu den entsprechenden Magnesiumhalogeniden. *Zeitschrift f ü r anorganische Chemie* **1948**, *256*, 25−36.
(32) Seifert, H.; Mueller, B.; Stoetzel, E. Thermochemische und strukturelle untersuchungen an systemen aus alkalimetalliodid un $MgI_2$ (1) bzw. $CaI_2$ (2). *Rev. Chim. Miner.* **1980**, *17*, 147−157.
(33) Grjotheim, K.; Holm, J. L.; Malmo, J. The Phase Diagram of the System $MgCl_2$-$CaCl_2$, and Thermo-dynamic Properties of Molten Mixtures in this System. *Acta Chem. Scand.* **1970**, *24*, 3802−3803.
(34) Matiašovskỳ, K. Phase diagrams of some systems important in electrolytic production of magnesium. I. Two-component systems $MgCl_2$-NaCl, $CaCl_2$-NaCl, and $MgCl_2$-$CaCl_2$. *Chem. Pap.* **1959**, *13*, 69−77.
(35) Abramov, G. The ternary system KCl-$MgCl_2$-NaCl. *Metallurg (Leningrad)* **1935**, *10*, 82−105.
(36) Speranskaya, E. Neobratimo-vzlimiaya sistema iz khloridov i sulfatov natriya i magniya. *Ivz. Akad. Nauk. SSSR, Ser. Khim* **1938**, 463−487.
(37) Menge, O. Die binaren Systeme von $Mgcl_2$ und $CaCl_2$ mit den Chloriden der Metalle K, Na, Ag, Pb, Cu, Zn, Sn und Cd. *Zeitschrift fur Anorganische und Allgemeine Chemie* **1911**, *72*, 162−219.
(38) Kleppa, O.; McCarty, F. Thermochemistry of Charge-Unsymmetrical Binary Fused Halide Systems. II. Mixtures of Magnesium Chloride with the Alkali Chlorides and with Silver Chloride. *J. Phys. Chem.* **1966**, *70*, 1249−1255.
(39) Johnson, C. E.; Hathaway, E. J. Solid-Liquid Phase Equilibria for the Ternary Systems Li(F, Cl, I) and Na(F, Cl, I). *J. Electrochem. Soc.* **1971**, *118*, 631.
(40) Amadori, M. Tendency of the halides and phosphates of the same metal to combine. I. Alkali chlorides and phosphates. *Atti della Accademia Nazionale dei Lincei. Memorie. Classe di Scienze Fisiche, Matematiche e Naturali. Serie VIII. Sezione II*, 1912, 182−188.
(41) Ilyasov, I.; Bergman, A. Ternary reciprocal systems of cadmium, caesium, potassium and sodium halides. *Russ. J. Inorg. Chem.* **1964**, *9*, 768−771.
(42) Oonk, H.; Blok, K.; van de Koot, B.; Brouwer, N. Binary common-ion alkali halide mixtures thermodynamic analysis of solid-liquid phase diagrams i. systems with negligible solid miscibility application of the extxd/sivamin method. *Calphad* **1981**, *5*, 55−74.
(43) Oonk, H. Solid-state solubility and its limits. The alkali halide case. *Pure Appl. Chem.* **2001**, *73*, 807−823.
(44) Melnichak, M.; Kleppa, O. Enthalpies of Mixing in the Binary Liquid Systems Alk(Cl−Br), Alk(Cl−I), and Alk(Br−I). *J. Chem. Phys.* **1972**, *57*, 5231−5241.
(45) Ilyasov, I.; Bostandzhiyan, A. The irreversible reciprocal system of chlorides and iodides of sodium and lead. *Soviet Research in Fused Salts, 1956, in English Translation*, 1958, 768−771.


https://doi.org/10.1021/acs.jpcc.4c07788
J. Phys. Chem. C 2025, 129, 2726−2738